A self-assembled leucine polymer sensitizes leukemic stem cells to chemotherapy by inhibiting autophagy in acute myeloid leukemia

Xi Xu,[1,2*] Jian Wang,[3*] Tong Tong,[4*] Wenwen Zhang,[2] Jin Wang,[2] Weiwei Ma,[5] Shunqing Wang,[5] Dunhua Zhou,[3] Jun Wu,[1,4] Linjia Jiang[1] and Meng Zhao[2]

[1]Guangdong Provincial Key Laboratory of Malignant Tumor Epigenetics and Gene Regulation, Sun Yat-sen Memorial Hospital, Sun Yat-sen University; [2]Key Laboratory of Stem Cells and Tissue Engineering (Ministry of Education), Zhongshan School of Medicine, Sun Yat-sen University; [3]Department of Pediatrics, Sun Yat-sen Memorial Hospital, Sun Yat-sen University; [4]Key Laboratory of Sensing Technology and Biomedical Instrument of Guangdong Province, School of Biomedical Engineering, Sun Yat-sen University and [5]Department of Hematology, Guangzhou First People's Hospital, School of Medicine, South China University of Technology, Guangzhou, Guangdong, China.

XX, JW and TT contributed equally as co-first authors.

Correspondence: M. Zhao
zhaom38@mail.sysu.edu.cn
L. Jiang
jianglj7@mail.sysu.edu.cn
J. Wu
wujun29@mail.sysu.edu.cn

Received: November 4, 2021.
Accepted: March 10, 2022.
Prepublished: March 17, 2022.

https://doi.org/10.3324/haematol.2021.280290

Abstract

Chemotherapy is the primary treatment option for acute myeloid leukemia (AML), but leukemic stem cells (LSC) can survive chemotherapy for disease recurrence and refractory. Here, we found that AML cells obtained from relapsed patients had increased autophagy levels than *de novo* AML cells. Furthermore, doxorubicin (DOX) treatment stimulated autophagy in LSC by repressing the mTOR pathway, and pharmaceutical inhibition of autophagy rendered chemoresistant LSC sensitive to DOX treatment in MLL-AF9 induced murine AML. Moreover, we developed a self-assembled leucine polymer, which activated mTOR to inhibit autophagy in AML cells by releasing leucine. The leucine polymer loaded DOX (Leu-DOX) induced much less autophagy but more robust apoptosis in AML cells than the DOX treatment. Notably, the leucine polymer and Leu-DOX were specifically taken up by AML cells and LSC but not by normal hematopoietic cells and hematopoietic stem/progenitor cells in the bone marrow. Consequently, Leu-DOX efficiently reduced LSC and prolonged the survival of AML mice, with more limited myeloablation and tissue damage side effects than DOX treatment. Overall, we proposed that the newly developed Leu-DOX is an effective autophagy inhibitor and an ideal drug to efficiently eliminate LSC, thus serving as a revolutionary strategy to enhance the chemotherapy efficacy in AML.

Introduction

Acute myeloid leukemia (AML) is a heterogeneous hematologic malignancy originating from hematopoietic stem/progenitor cells with gene mutations and genomic rearrangements.[1,2] The chromosomal translocation at t(9;11)(p22;q23) that encodes the MLL (mixed-lineage leukemia)-AF9 fusion protein was detected in AML patients with poor prognosis.[3,4] The traditional 7+3 chemotherapy regimen, consisting of 7 days of cytarabine (Ara-C) and 3 days of doxorubicin (DOX), remained the standard treatment against AML for decades.[5-7] However, less than 50% of AML patients achieve an overall 5-year survival after initial remission[8-10] due to the chemoresistant leukemic stem cells (LSC) that survive chemotherapy and generate progeny leukemic cells for disease recurrency through multiple mechanisms.[11-14]

Autophagy is an important cell survival mechanism that senses the cellular metabolic stress to provide energy and molecular structure by digesting and recycling damaged cellular components through lysosomes.[15-17] Multiple intracellular and extracellular stress signals, including metabolic stress, hypoxia, redox stress, and immune signals, induce autophagy, which alters chemotherapeutic responses in solid tumor cells.[18] For example, gut microbiota regulates autophagy through inflammation pathways for chemoresistance in colorectal cancer.[19] Co-treatment with chemotherapy and autophagy inhibitor overcomes the chemoresistance in hepatoma carcinoma cells.[20] Depletion of the autophagy-key regulator, Atg5 or Atg7, re-

duces functional leukemia-inhibiting cells and enhances the efficacy of chemotherapy drugs in AML treatment.[21] Pharmaceutical inhibition of autophagy is also suggested to improve chemotherapy efficacy in leukemia cells.[22] However, a therapeutic approach to inhibit autophagy and improve chemotherapy efficacy in eliminating LSC for AML treatment remains undeveloped.

The mTOR complex 1 (mTORC1) acts as the master regulator of autophagy by regulating various processes of autophagosome formation.[23] Deprivation of nutrients, growth factors, or cellular energy, inhibits mTORC1 activity to induce autophagy.[24] Branched-chain amino acids, especially leucine, are effective autophagy repressors by activating the mTORC1 complex.[25-28] Therefore, inhibition of autophagy by leucine might be a rational strategy to enhance the chemotherapy efficacy to eradicate the chemoresistant LSC, thus overcoming disease recurrence. Here, we developed a novel self-assembled leucine polymer (8L6) as a functional drug carrier that specifically targeted LSC in the bone marrow (BM) to inhibit their autophagy levels in AML mice. Furthermore, we developed a leucine polymer-loaded doxorubicin (Leu-DOX) to improve the DOX efficacy in eliminating LSC in preclinical AML models.

Methods

Acute myeloid leukemia model and *in vivo* treatment

C57BL/6J mice were purchased from the Laboratory Animal Center of Sun Yat-sen University. For the AML murine model, MSCV-MLL-AF9-IRES-GFP infected preleukemic cells ($4x10^5$) were intravenously injected into lethally irradiated (9 Gy) recipients (6–8-weeks old) together with $1x10^5$ rescue cells. For chemotherapy, cytarabine (Ara-C, HY-13605, MCE) at 100 mg kg^{-1} bodyweight, and doxorubicin (DOX, HY-15142A, MCE) at 3 mg kg^{-1} bodyweight, were intravenously injected into AML mice for a 5-day-treatment protocol (3-day-DOX and 5-day-Ara-C). For DOX treatment, DOX or Leu-DOX were intravenously injected into AML mice at 3 mg kg^{-1} bodyweight for 3 consecutive days as indicated. Chloroquine (CQ) was intravenously injected into AML mice at 50 mg kg^{-1} bodyweight for 5 consecutive days as indicated. The numbers of animals used per experiment are shown in the figure legends. All animal experiments were performed according to protocols approved by the Institutional Animal Care and Use Committee.

Cell culture and *in vitro* treatment

THP-1 cells were cultured in RPMI 1640 with 10% fetal bovine serum and 2 mM glutamine. Murine AML cells were cultured in StemSpan™ serum-free expansion medium (SFEM) (09650, STEMCELL™ Technologies) supplemented with 50 ng ml^{-1} SCF (Peprotech), 10 ng mL^{-1} TPO (Peprotech), 10 ng mL^{-1} IL-3 (Peprotech), and 10 ng mL^{-1} IL-6 (Peprotech). Cells were treated with DOX (1 μM), Leu-DOX (1 μM), DOX@PLGA (1 μM), 8L6 (10 μM), CQ (HY-17589A, MCE, 10 μM), rapamycin (HY-10219, MCE, 10 nM) where indicated. Cell proliferation fold changes were calculated by the ratio between the cell numbers at indicated time points after treatments compared to cell numbers before treatment. For apoptosis analysis, cells were stained by Annexin V* ROMAN (640907, Biolegend) and further incubated with 0.01 μg μL^{-1} Dapi (1306, Thermo Fisher Scientific) or 7-AAD (00699350, eBioscience) for 30 minutes (min) at room temperature. For γ-H2AX and LC3 staining, the cells were transferred to a glass slide and allowed to stand for 1 hour (h) to make the cells adhere to the glass slide. After fixation with 4% paraformaldehyde for 15 min, cells were permeabilized with 0.5% Triton X-100 at room temperature for 30 min, blocked with 10% goat serum solution at room temperature for 1 h, washed, and incubated with anti-γ-H_2AX primary antibody (rabbit, 1:100, 613404, Biolegend) and LC3 primary antibody (rabbit, 1:100, 4108S, Cell Signaling Technology) for overnight. After that, the secondary antibody was added dropwise and incubated at room temperature for 1 h, and the high-speed confocal imaging system (Dragonfly CR-DFLY-202 2540, Andor) was used for imaging.

Synthesis of leucine polymer (8L6)

The leucine polymer was synthesized through three steps: (1) The monomer-1 (N8, dip-nitrophenyl ester of dicarboxylic acids) was synthesized from the reaction of di-p-nitrophenol and succinyl chloride; (2) the monomer-2 (Leu-6, toluenesulfonic acid salt of L-leucine) was obtained from the reaction between L-leucine and 1,6-hexylene glycol; (3) the leucine polymer (8L6) was synthesized from the polycondensation of monomer-1 and monomer-2. Other methods are described in the *Online Supplementary Appendix*.

Results

Autophagy protects leukemic stem cells from chemotherapy in acute myeloid leukemia

In order to investigate the autophagy pathways, we analyzed the clinical response and gene expression profile of AML patients from the Therapeutically Applicable Research To Generate Effective Treatments (TARGET) dataset, which included the remission group (n=91), relapse group (n=163), and death group (n=41). The gene set enrichment analysis (GSEA) showed that autophagy-related genes were significantly more enriched in the relapsed group than in the remission group (Figure 1A), indicating that autophagy might be involved in the disease recurrence after chemotherapy. We then compared the ex-

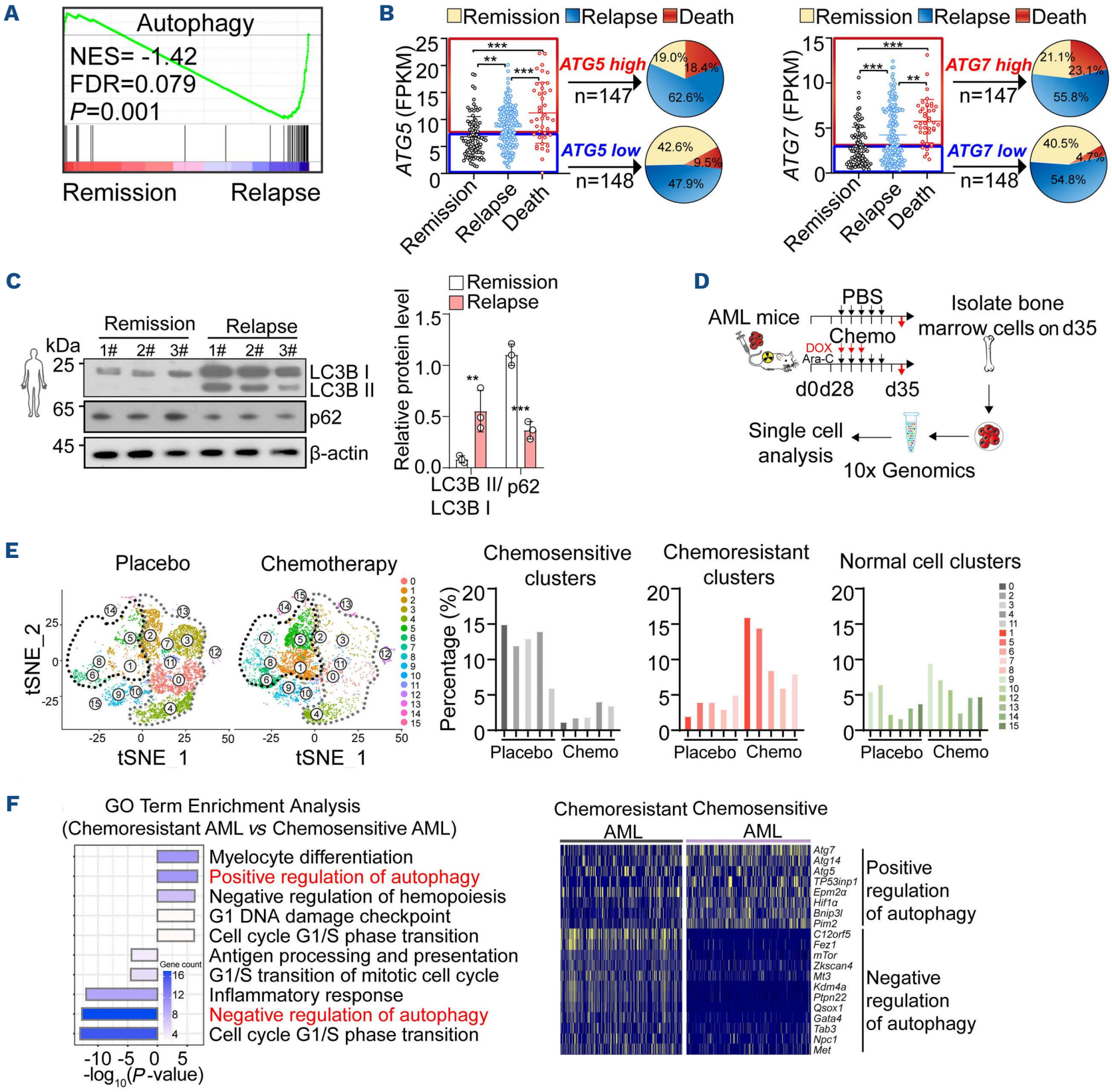

Figure 1. Autophagy activity is high in chemoresistant acute myeloid leukemia cells. (A) Gene set enrichment analysis of autophagy pathways in acute myeloid leukemia (AML) patients with remission or relapse. (B) Distribution of ATG5 (left) and ATG7 (right) expression in AML patients. (C) Western blots (left) and quantification (right) of LC3B and p62 in primary-diagnosed and relapsed AML patients. 1#, 2#, 3# indicate 3 individual patients. (D) Schematic depicting the strategy to analyze murine AML cells by single-cell RNA-sequencing. Chemotherapy (chemo) included doxorubicin (DOX) and cytarabine (Ara-C) treatments. (E) tSNE (left) and quantification of clusters (right) of bone marrow cell from AML mice with chemotherapy (right, n=5 mice) or placebo (left, n=5 mice) treatment. (Black circle: chemoresistant leukemic cell clusters; grey circle: chemosensitive leukemic cell clusters). (F) Gene ontology (GO) analysis of pathways enriched in chemoresistant AML cells compared to chemosensitive AML cells (left) and differentially-expressed autophagy-related genes in chemosensitive AML cells and chemoresistant AML cells (right).

pression of canonical autophagy genes, ATG5, ATG7, and microtubule-associated protein light chain 3B-II (LC3B-II) in each group. AML patients with higher ATG5 or ATG7 expression had a higher risk of relapse and cancer-related death after chemotherapy (Figure 1B). The protein levels of LC3B-II were higher, but autophagy targeted LC3 interacting protein p62/SQSTM1 (p62)[29] levels were lower in specimens from relapsed AML patients compared to remission AML patients, indicating autophagy activity is higher in relapsed samples (Figure 1C).

We next investigated how chemotherapy influences leukemic cell transcriptional profile at single-cell resolution. We transduced wild-type BM with retrovirus expressing MLL-AF9 to recapitulate aggressive human

t(9;11)$^+$ AML in mice.[30] Using single-cell RNA sequencing (scRNA-seq), we profiled the AML cells in BM 2 days after Ara-C and DOX combined chemotherapy or placebo treatment (Figure 1D). Unbiased clustering of the BM cells from AML mice defined 16 clusters with three major groups: chemoresistance leukemic cell clusters (cluster 1, 5, 6, 7, and 8), chemosensitive leukemic cell clusters (cluster 0, 2, 3, 4, and 11), and the normal hematopoietic cell clusters (cluster 9, 10, 12, 13, 14, and 15) (Figure 1E). Gene ontology (GO) analysis revealed that chemoresistance leukemia cell clusters had distinguished pathways in the cell cycle, myelocyte differentiation, and autophagy compared to chemosensitive leukemia cell clusters (Figure 1F). Notably, autophagy-related genes were significantly enriched in chemoresistance leukemia cells than in chemosensitive leukemic cells (Figure 1F).

We further investigated the autophagy levels in AML cells after chemotherapy treatment in AML mice. We found that phosphorylated mTOR, S6, 4EBP1 decreased, but LC3B-II increased in the LSC-enriched cells (GFP$^+$c-KIT$^+$, GFP co-expressed from the MLL-AF9-carrying retrovirus)[31] obtained from MLL-AF9 induced AML mice (hereafter referred as to AML mice) 2 days after chemotherapy treatment *in vivo* (Figure 2A). These results indicated that chemotherapy might inhibit the mTOR pathway to stimulate autophagy in LSC. Next, we investigated the potential function of autophagy in chemotherapeutic responses by pharmaceutically inhibiting autophagy using autophagy inhibitor chloroquine (CQ), a lysosome inhibitor blocking downstream effects of autophagy, in purified GFP$^+$c-KIT$^+$ cells from AML mice for *in vitro* treatment. We found that the cell proliferation rate was significantly decreased in the DOX treatment group when CQ was administrated (CQ 21.4% decrease, DOX 40.2% decrease, DOX+CQ 78.9% decrease, Figure 2B). More importantly, autophagy inhibition dramatically increased the DOX-induced apoptosis in GFP$^+$c-KIT$^+$ cells compared to DOX treatment (Figure 2C). Furthermore, we explored the effect of CQ treatment *in vivo* (Figure 2D). Consistent with the *in vitro* observations, DOX *in vivo* treatment increased LC3B-II and decreased p62 to activate the autophagy pathway in AML cells. However, CQ treatment attenuated the activation of the autophagy pathway in AML cells induced by DOX treatment in AML mice (Figure 2E). Consequently, combined treatment with DOX and CQ more efficiently reduced the leukemic burden in peripheral blood of AML mice than DOX treatment (Figure 2F).

Overall, these data indicated that chemotherapy stimulated autophagy in LSC, and inhibition of autophagy increased the efficacy of chemotherapy to more efficiently reduce chemoresistant LSC.

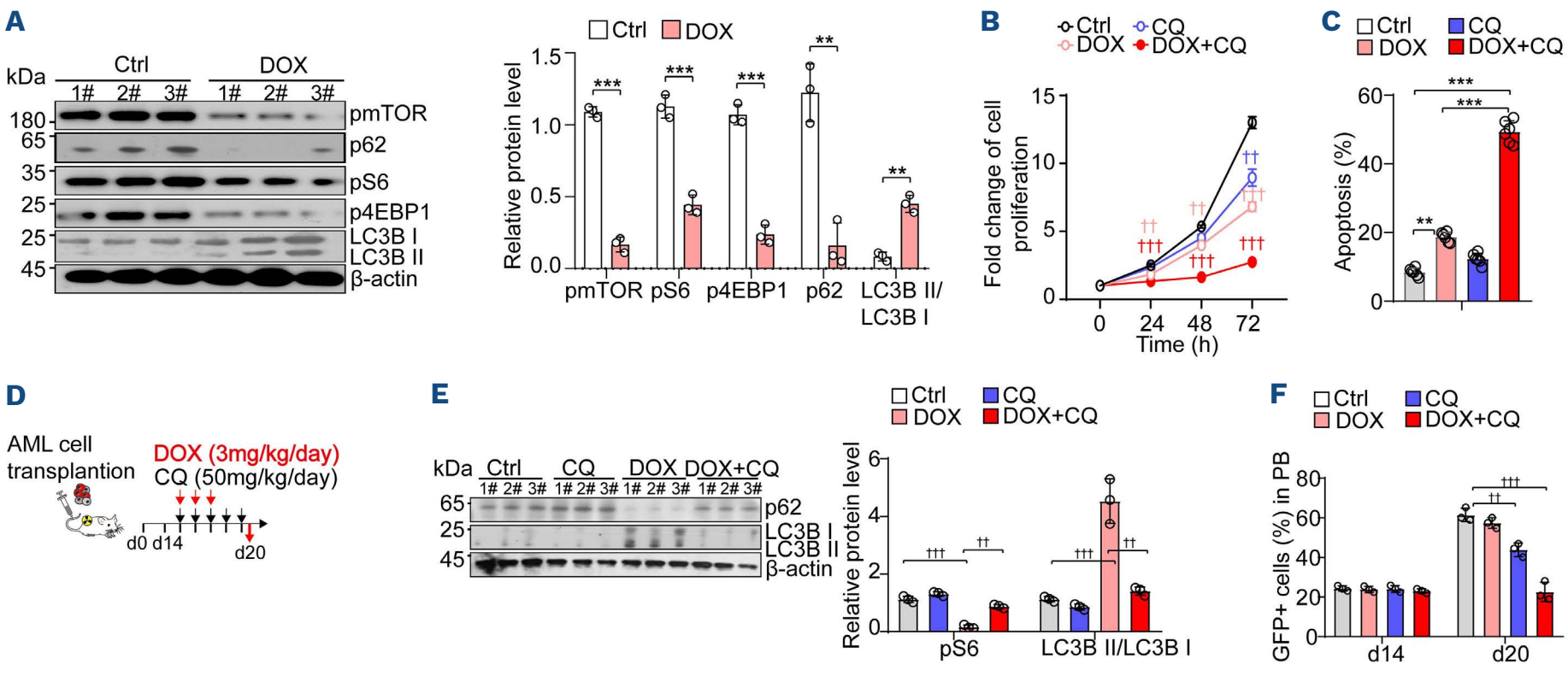

Figure 2. Autophagy protects leukemic stem cells from chemotherapy in acute myeloid leukemia. (A) Western blots (left) and quantification (right) of the mTOR pathway and LC3B in GFP$^+$c-KIT$^+$ cells from acute myeloid leukemia (AML) mice bone marrow (BM) 2 days after chemotherapy or placebo treatment as indicated. 1#, 2#, 3# indicate 3 individual AML mice. Chemotherapy (chemo) included doxorubicin (DOX) and cytarabine (Ara-C) treatments. (B) The cell proliferation rate of isolated GFP$^+$c-KIT$^+$ cells with indicated *in vitro* treatment (n=5 mice per group). GFP$^+$c-KIT$^+$ cells were purified from AML mice 2 days after indicated treatment. (C) The apoptosis rate of GFP$^+$c-KIT$^+$ cells at 72 hours (h) after indicated *in vitro* treatment (n=6 replicates from 3 mice per group). (D) Schematic depicting the treatment strategy for AML mice. (E) Western blots (left) and quantification (right) of the p62 and LC3B in isolated GFP$^+$c-KIT$^+$ cells from the BM of AML mice received DOX and CQ treatment as indicated. (F) The percentage of GFP+ leukemic cells in peripheral blood with indicated treatments (n=3 mice).

Leucine polymer-loaded doxorubicin specifically targets leukemic cells but spares normal tissues in acute myeloid leukemia mice

As the branched-chain amino acids, especially leucine, can inhibit autophagy by activating mTOR,[32,33] we proposed that self-assembled leucine polymer might facilitate chemotherapy by inhibiting autophagy. Therefore, we synthesized the leucine polymer, 8L6 (*Online Supplementary Figure S1A*), and loaded DOX in 8L6 to generate Leu-DOX for the first time. The average size of Leu-DOX was 104.3±1.19 nm with a narrow polydispersity index (*Online Supplementary Figure S1B*). Leu-DOX showed a uniform spherical shape under the electron microscope (*Online Supplementary Figure S1C*). The encapsulation efficiency and drug loading of DOX in Leu-DOX detected by fluorescence spectrophotometry were 58.9±0.3% and 5.9%±0.03%, respectively *(Online Supplementary Figure S1D*). The particle size of Leu-DOX did not change significantly after long-term storage *in vitro*, indicating the favorable stability of Leu-DOX (*Online Supplementary Figure S1E*). Considering that Leu-DOX will transport through different pH environments in the body,[34] we incubated Leu-DOX in a series of pH solutions to examine the release efficiency. The release of DOX at pH 5.0 was significantly higher than at pH 7.4 (*Online Supplementary Figure S1F*), suggesting that Leu-DOX might rapidly release DOX in the acid tumor microenvironment.

Drug internalization and persistent retention are critical for cancer treatment.[35] In order to explore the uptake of Leu-DOX by AML cells, we treated THP-1, a human *MLL-AF9*$^{+}$ AML cell line,[36] with DOX or Leu-DOX and measured the DOX uptake by characterizing the DOX-inherited red fluorescence.[37] Notably, Leu-DOX achieved higher DOX content in THP-1 cells than free DOX after incubation (Figure 3A), although DOX and Leu-DOX represented similar inherent fluorescent intensity (*Online Supplementary Figure S2A*). Flow cytometry analysis of the DOX fluorescence intensity further confirmed the higher drug content in THP-1 cells with Leu-DOX treatment than with DOX treatment (Figure 3B).

In order to evaluate the biodistribution of Leu-DOX *in vivo*, we intravenously injected DiR, a near-infrared dye for *in vivo* imaging or DiR@8L6, and imaged the dynamic bioluminescence levels in AML mice (*Online Supplementary Figure S2B*). The fluorescence intensity of free DiR accumulated in the epigastrium peaking at 24 h, but dim DiR signals were detected in the BM of the femur and tibia, indicating a low drug delivery efficiency in the BM. In contrast, the DiR@8L6 had a 6.92-fold increased accumu-

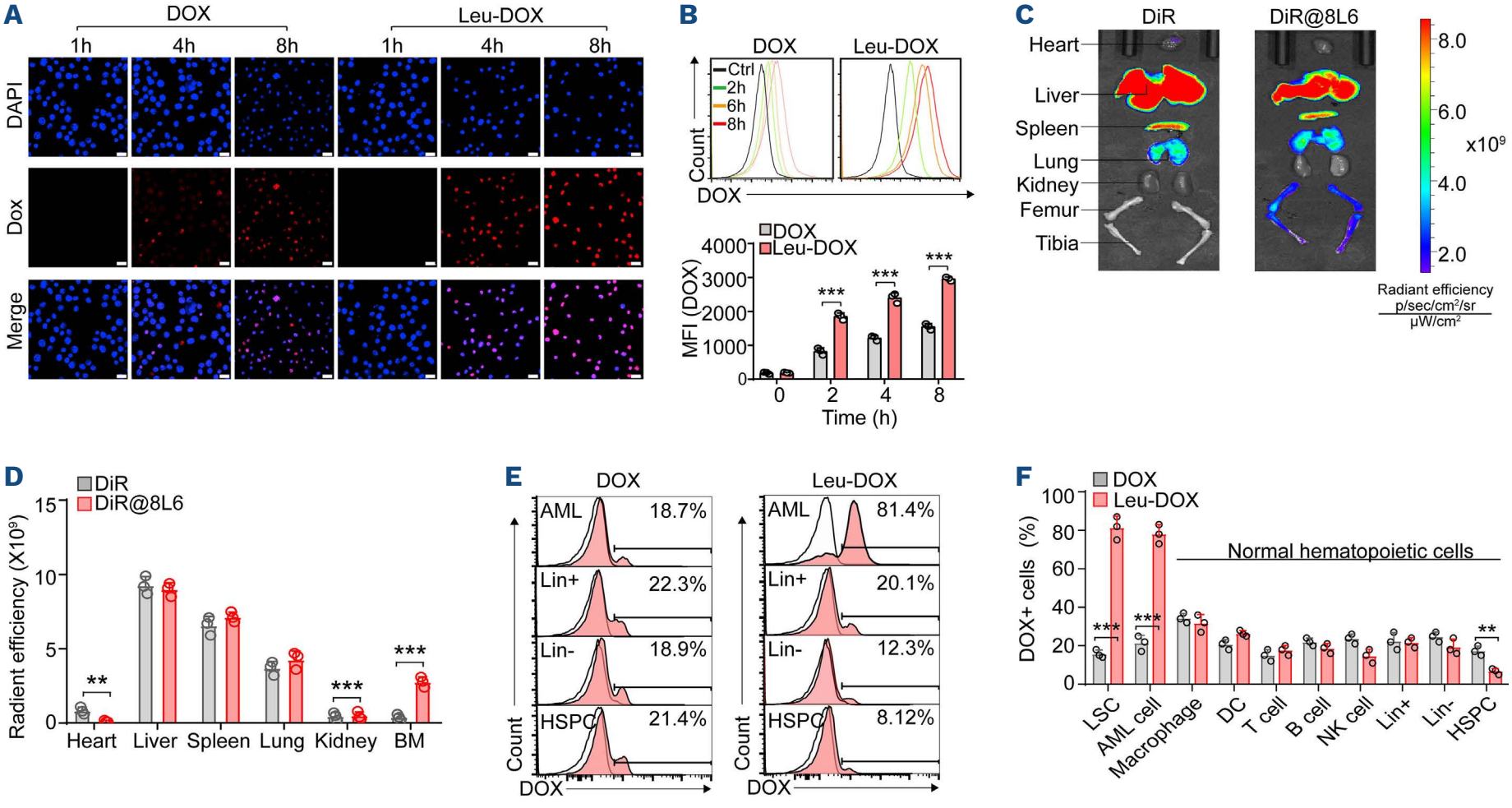

Figure 3. Leucine polymer-loaded doxorubicin specifically targets leukemic cells but spares normal tissues in acute myeloid leukemia mice. (A) Images of THP-1 cells with doxorubicin (DOX) or leucine polymer-loaded doxorubicin (Leu-DOX) treatment for the indicated time (scale bar=20 μm). (B) Representative flow cytometry profile (up) and quantitative cellular uptake (down) of DOX in THP-1 cells incubated with DOX or Leu-DOX for the indicated time. (C and D) The fluorescence images (C) and quantification (D) of DiR in the indicated organs of acute myeloid leukemia (AML) mice 24 hours (h) after DiR or DiR@8L6 injection. (E and F) Representative flow cytometry profile (E) and quantitative (F) of the intensity of DOX fluorescence in different hematopoietic cell populations of AML mice. The DOX fluorescence was quantified 4 h after injection (n=3 mice per group).

lation in the BM than free DiR, an 84.8% decrease in the heart at 48 h after injection, suggesting that 8L6 might be an efficient drug carrier for leukemic treatment with reduced tissue damage (Figure 3C and D).

In order to further evaluate the cellular targeting specificity of Leu-DOX within the BM of AML mice, we examined the fluorescence intensity in various cell populations in the BM of AML mice using *in vivo* cell trace. Notably, Leu-DOX targeted over 80% of leukemic cells and GFP^+ckit^+ LSC-enriched cells. Conversely, Leu-DOX targeted ~20-40% of normal mature hematopoietic cells, such as macrophages, dendritic cells (DC), T cells, B cells, and natural killer (NK) cells, and much fewer hematopoietic stem and progenitor cells (~7.89%) in the BM of AML mice. However, DOX had no cell type specificity. (Figure 3E and F). These observations indicated that Leu-DOX specifically targets AML cells but spares normal hematopoietic cells. We consistently observed the similar leukemic cell targeting efficiency of Dil@8L6 compared to free Dil (red fluorescence better for single-molecule imaging) (*Online Supplementary Figure S2C* and *D*), indicating that 8L6 might be an efficient and specific drug carrier for AML treatment.

Leucine polymer-loaded doxorubicin enhances the chemotherapy efficacy for acute myeloid leukemia cells *in vitro*

In order to explore the therapeutic effects of Leu-DOX *in vitro*, we treated THP-1 cells with 8L6, DOX, and Leu-DOX, respectively. Our data showed that Leu-DOX inhibited THP-1 cell proliferation more efficiently than DOX treatment (Figure 4A). Furthermore, Leu-DOX induced more dramatic apoptosis in THP-1 cells than DOX treatment at 48 h after treatment (Figure 4B). Since DOX blocks topoisomerase 2 to trigger DNA damage,[38] we further showed that Leu-DOX treated THP-1 cells had much more DNA damage than THP-1 cells with DOX treatment examined by the intensity of γH2AX (Figure 4C) and comet assay (*Online Supplementary Figure S3*).

In order to exclude the possibility that increased cell toxicity of Leu-DOX was mainly due to nanoparticle facilitated cell uptake efficacy, we compared 8L6 with another Food and Drug Administration (FDA) approved drug nanocarrier PLGA (polylactic-co-glycolic acid).[39] DOX@PLGA and Leu-DOX showed comparable increased cellular uptake of DOX than free DOX in THP-1 cells (Figure 4D), indicating the enhanced drug delivery efficiency in AML cells of these two drug carriers. However, DOX@PLGA showed less advantage in inhibiting cell growth and inducing apoptosis of THP-1 cells than Leu-DOX (Figure 4E and F), suggesting that 8L6 might facilitate chemotherapy more than a canonical drug carrier for AML treatment.

Leucine polymer-loaded doxorubicin inhibits autophagy to enhance chemotherapy efficacy in acute myeloid leukemia cells

As leucine can activate the mTORC1 complex to inhibit

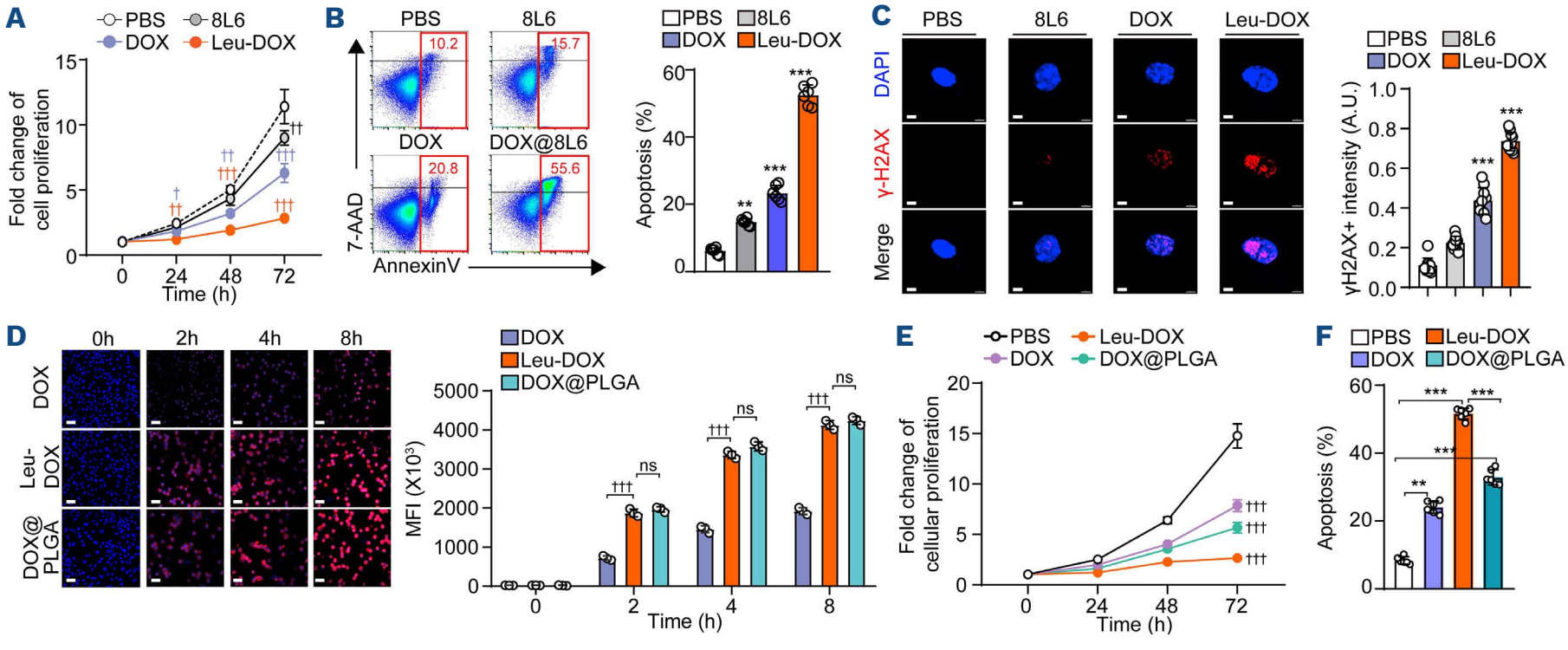

Figure 4. Leucine polymer-loaded doxorubicin enhances the chemotherapy efficacy for acute myeloid leukemia cells *in vitro*. (A) The cell proliferation rate of THP-1 cells treated with phospate-buffered saline (PBS) (control [Ctrl]), 8L6, doxorubicin (DOX), or leucine polymer-loaded doxorubicin (Leu-DOX) as indicated (n=5 independent replicates per group). (B) Representative fluorescence activated cell sorting plots (left) and the quantification (right) of Annexin V^+ apoptotic THP-1 cells 48 hours (h) after treatment (n=6 replicates). (C) Representative Images (left) and quantification (right) of the γ-H2AX intensity in THP-1 cells 48 h after indicated treatment (scale bar=1 μm) (n=6 replicates). (D) Representative Images (left) and quantification (right) of DOX fluorescent signal in THP-1 cells at indicated time after treatment with DOX, Leu-DOX, or DOX@polylactic coglycolic acid (PLGA) (scale bar=20 μm). (E) The cell proliferation rate of THP-1 cells treated with PBS (Ctrl), DOX, Leu-DOX, and DOX@PLGA. (n=5 independent replicates per group). (F) Apoptotic THP-1 cells at 72 h after indicated treatment (n=6 independent replicates per group).

autophagy,[40] we further investigated the role of 8L6 and Leu-DOX in regulating autophagy in AML cells. Intriguingly, we found that Leu-DOX did not repress the mTORC1 pathway and induce autophagy as DOX treatment did in THP-1 cells after *in vitro* treatment, examined by the pmTOR, pS6, and p4EBP, LC3B-II, and LC3 puncta (Figure 5A and B; *Online Supplementary Figure S4A*), indicating that Leu-DOX might enhance the efficacy of DOX treatment by inhibiting autophagy. In line with this, we found that inhibiting autophagy in THP-1 cells by lentivirus-mediated ATG5 knockdown (Figure 5C and D; *Online Supplementary Figure S4B*) improved the cell growth inhibition and apoptosis-inducing effects of DOX treatment to similar levels as Leu-DOX treatment (Figure 5E and F). By contrast, inhibiting the mTORC1 pathway by rapamycin (*Online Supplementary Figure S4C* and *D*) increased autophagy (*Online Supplementary Figure S4E*), which compromised the growth inhibition and apoptosis-inducing effects of Leu-DOX treatment to the similar levels as DOX treatment in THP-1 cells (*Online Supplementary Figure S4F* and *G*).

Leucine polymer-loaded doxorubicin inhibits autophagy and reduces leukemic stem cell frequency *in vivo*

In order to investigate the effects of Leu-DOX for AML treatment *in vivo*, we started the treatment 14 days after transplantation when the chimeric rate of leukemia cells (GFP^+) reached about 15% in the peripheral blood of AML mice (Figure 6A). Leu-DOX treatment dramatically reduced the frequency, and absolute numbers of LSC-enriched cells due to increased apoptosis in the BM of AML mice, including $GFP^+c\text{-}KIT^+$ cells, $GFP^+Lin^-Sca1^-c\text{-}KIT^+CD34^+FcgRII/III^+$ (L-GMP) cells[41] (Figure 6B and E), $GFP^+Lin^-Sca1^+c\text{-}KIT^+$ (LSK) cells (*Online Supplementary Figure S5A* to *C*), and $GFP^+Lin^-Sca1^-c\text{-}KIT^+$ (LK) cells (*Online Supplementary Figure S5D* to ^{F}).[42] Conversely, we also noticed that DOX treatment triggered apoptosis and reduced the absolute number of LSC-enriched cells but enriched their frequency in the BM of AML mice (Figure 6B to E; *Online Supplementary Figure S5*).

Our data showed that DOX treatment for AML mice significantly inactivated the mTOR pathway to induce autophagy in LSC enriched $GFP^+c\text{-}KIT^+$ cells, examined by the increased LC3B-II and reduced p62. However, Leu-DOX treatment did not affect the mTOR pathway or influence autophagy protein LC3B-II and p62 levels in $GFP^+c\text{-}KIT^+$ cells (Figure 6F). In line with this, Leu-DOX dramatically reduced the colony-forming leukemic cells in the BM of AML mice and compromised their self-renewal capacity in

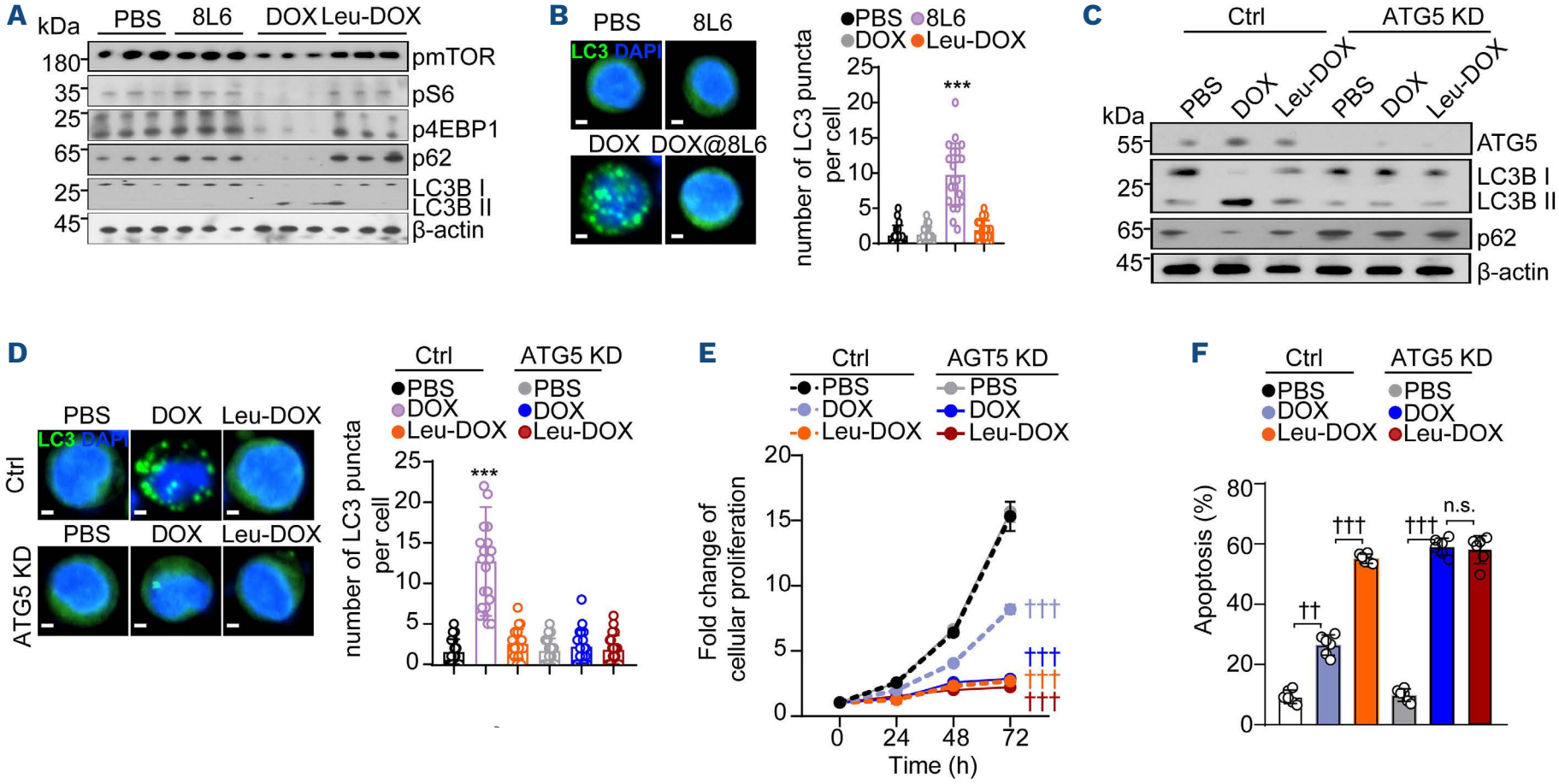

Figure 5. Leucine polymer-loaded doxorubicin inhibits autophagy to enhance chemotherapy efficacy in acute myeloid leukemia cells. (A) Western blots of the mTOR pathway, LC3B and p62 in THP-1 cells 48 hours (h) after indicated treatment. (n=3 independent replicates per group). (B) Representative image (left) and quantification (right) of LC3 puncta in THP-1 cells 48 h after treatment (scale bar=3 μm) (n=20 cells). (C) Western blots of the AGT5, LC3B, and p62 in control and ATG5 KD THP-1 cells 48 h after indicated treatment. (D) Representative images (left) and quantification (right) of LC3 puncta in control and ATG5 KD THP-1 cells 48 h after indicated treatment (scale bar=2 μm) (n=20 cells). (E) The cell proliferation rate of control and ATG5 KD THP-1 cells after indicated treatment. (n=6 replicates). (F) The apoptosis rate of control and ATG5 KD THP-1 cells 72 h after indicated treatment, knockdown (KD) (n=6 replicates).

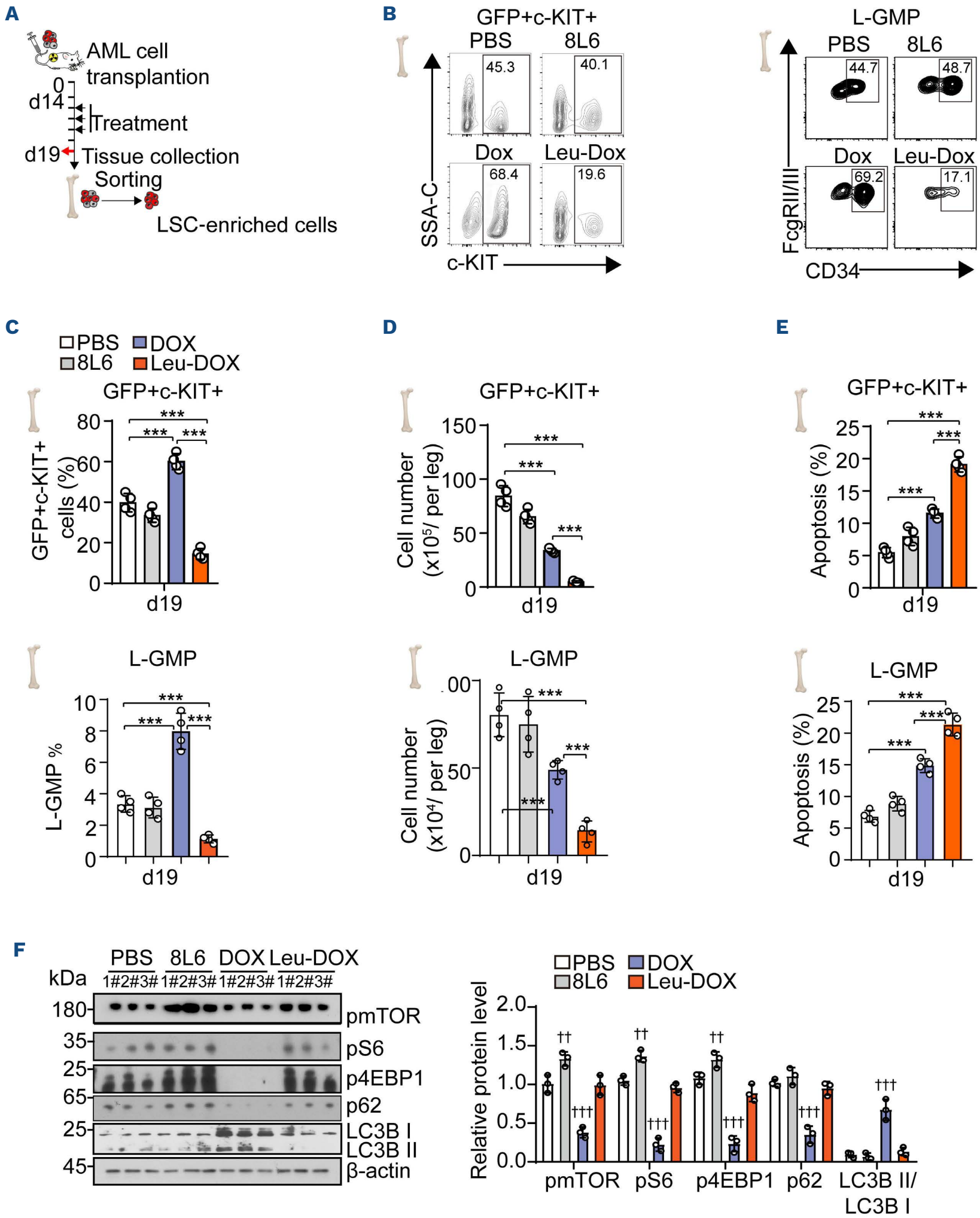

Figure 6. Leucine polymer-loaded doxorubicin inhibits autophagy and reduces leukemic stem cell-enriched cells in acute myeloid leukemia mice. (A) Schematic of drug treatment and analysis. (B) Representative fluorescence activated cell sorting (FACS) plots of GFP⁺c-KIT⁺ cells (left) and GFP⁺Lin⁻Sca1⁻c-KIT⁺CD34⁺FcgRII/III⁺ cells (right, L-GMP) in the bone marrow (BM) of acute myeloid leukemia (AML) mice 2 days after indicated treatments. (C) The frequency of GFP⁺c-KIT⁺ cells (up) and GFP⁺Lin⁻Sca1⁻c-KIT⁺CD34⁺FcgRII/III⁺ cells (down) in the BM of AML mice 2 days after indicated treatments (n=4 mice). (D) The absolute number of GFP⁺c-KIT⁺ cells (up) and GFP⁺Lin⁻Sca1⁻c-KIT⁺CD34⁺FcgRII/III⁺ cells (down) in the BM of AML mice 2 days after indicated treatments (n=4 mice). (E) The apoptosis rate of GFP⁺c-KIT⁺ cells (up) and GFP⁺Lin⁻Sca1⁻c-KIT⁺CD34⁺FcgRII/III⁺ cells (down) in the BM of AML mice 2 days after indicated treatments (n=4 mice). (F) Western blots (left) and quantification (right) of mTOR pathway, LC3B, and p62 in GFP⁺c-KIT⁺ cells from AML mice 2 days after indicated treatment. 1#, 2#, 3# indicate 3 individual AML mice.

serial plating assay (81.6% reduction in the primary plating, 89.9% reduction in the secondary plating). However, DOX treatment enriched the frequency of colony-forming cells in an equal number of BM cells from AML mice than mice receiving placebo treatment (1.72-fold increase in the primary plating, 1.56-fold increase in the secondary plating) (Figure 7A and B). In order to investigate how Leu-DOX treatment impacts functional LSC *in vivo*, we further performed a limiting dilution assay using BM cells from AML mice 2 days after DOX, Leu-DOX, or placebo treatment (Figure 7C). We found that Leu-DOX treatment dramatically reduced the frequency of functional LSC in the BM of AML mice. Notably, Leu-DOX treatment reduced ~1,000-fold functional LSC (1/58) in the BM of AML mice than AML mice received DOX treatment (1/50,385) (Figure 7D to F).

Leucine polymer-loaded doxorubicin enhances the chemotherapy efficacy in acute myeloid leukemia mice with reduced tissue toxicity

We further investigated the therapeutic efficacy of Leu-DOX in treating AML mice (Figure 8A). Leu-DOX treatment robustly reduced the leukemia burden in peripheral blood (73.6% decrease on d21, and 64.3% decrease on d28), which was much more efficient than DOX treatment alone (36.8% decrease on d21, and 29.9% decrease on d28) (Figure 8B). Blood smear assay showed that Leu-DOX-treated group had much fewer immature leukemic cells than DOX or placebo groups (Figure 8C).

Leu-DOX treatment also more efficiently recovered the bodyweight of AML mice than DOX treatment (*Online Supplementary Figure S6A*) compared to placebo treatment, indicating the reduced tissue toxicity in Leu-DOX treated mice. DOX exhibits toxicity in the heart, liver, kidney, and nervous tissue, which causes severe complications in AML patients receiving standard chemotherapy in clinical.[43-45] Our data showed that Leu-DOX treatment caused much less side effect toxicity in the structural integrity and reduced leukemic cell infiltration in the heart, liver, spleen, lung, and kidney than DOX treatment in AML mice (*Online Supplementary Figure S6B* to *D*).

Furthermore, Leu-DOX significantly reduced the leukemia burden in BM (68.7% reduction) than placebo treatment, which was much more efficient than the DOX treatment (31.8% reduction) (Figure 8D). Consistently, Leu-DOX more efficiently reduced the weight of the liver and spleen, which were infiltrated with leukemic cells in AML mice (61.9% reduction spleen and 37.3% reduction liver) than DOX treatment (39.4% reduction spleen, and 24.4% reduction liver, Figure 8E). More importantly, the Leu-DOX treatment significantly prolonged the overall survival of AML mice than AML mice receiving placebo or DOX treatment (Figure 8F).

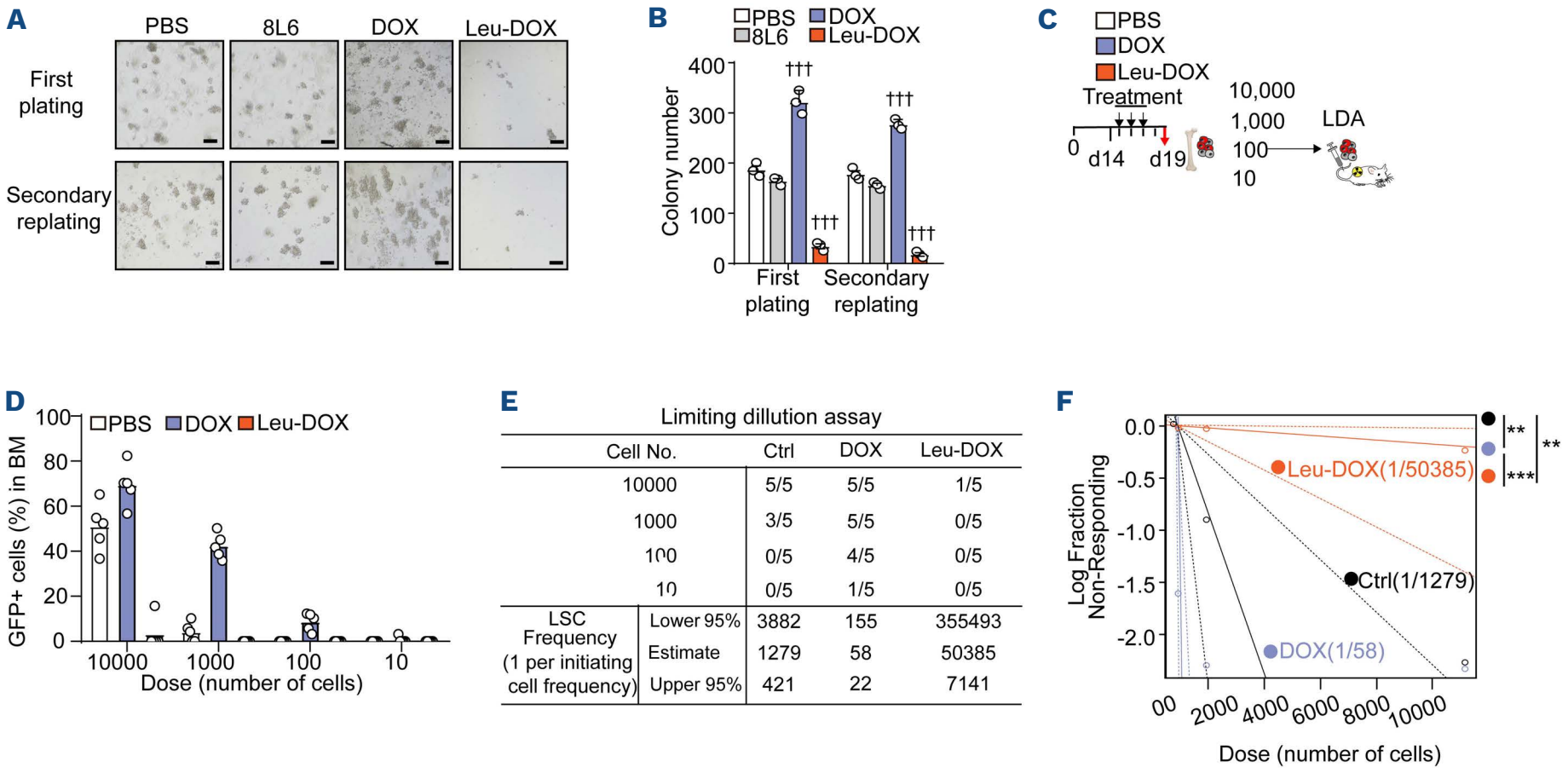

Figure 7. Leucine polymer-loaded doxorubicin reduces leukemic stem cells in acute myeloid leukemia mice. (A and B) Representative images (A) and quantification (B) of colony-forming cells in the bone marrow (BM) of acute myeloid leukemia (AML) mice 2 days after indicated treatments. (C) Schematic illustration of limited dilution assay of BM cells of AML mice 2 days after indicated treatments. (D and F) The percentage of GFP^+ leukemic cells in peripheral blood (D), the quantification of morbidity in recipients (E), and competitive repopulating unit (CRU) analysis for the leukemic stem cell (LSC) frequency (F) (n=5 mice per group).

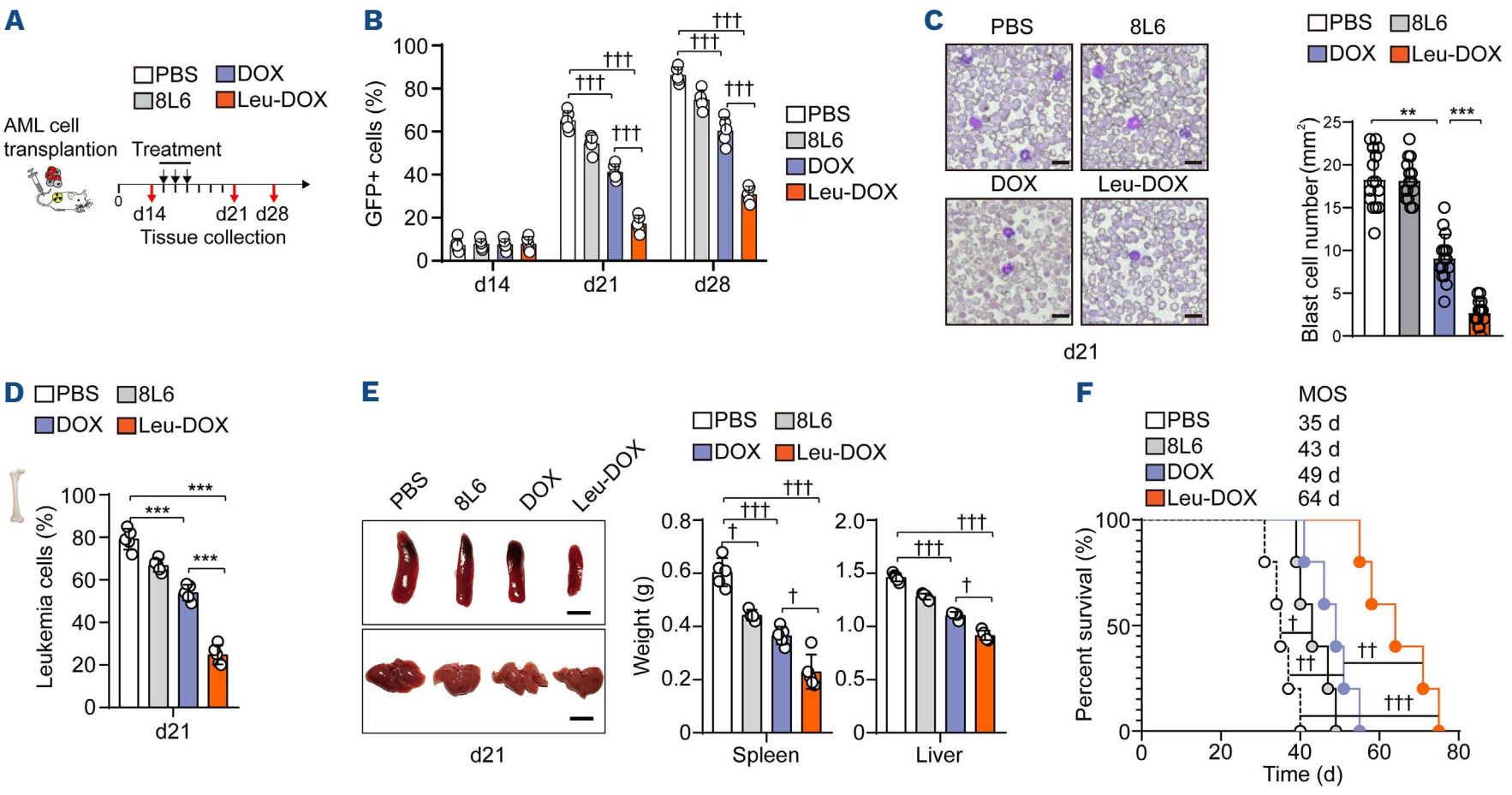

Figure 8. Leucine polymer-loaded doxorubicin enhances the chemotherapy efficacy in acute myeloid leukemia mice. (A) Schematic of acute myeloid leukemia (AML) mouse treatment. (B) The percentage of GFP⁺ leukemic cells in peripheral blood at the indicated time after treatment. (C) Representative peripheral blood smear (left) and quantification (right) of blast cells in the peripheral blood smear from AML mice at day 21 (d21) with indicated treatment (n=15 replicates from 5 mice). (D) The percentage of GFP⁺ leukemic cells in the bone marrow (BM) of AML mice at d21 with indicated treatment (n=5 mice). (E) Images (left) and weight of spleen and liver (right) of AML mice at d21 with indicated treatment (n=5 mice) (scale bar=1 cm). (F) The survival curve of AML mice with indicated treatments (n=5 mice). MOS: median overall survival.

Discussion

Autophagy plays an essential role in normal hematopoietic stem cell maintenance.[46,47] Depletion of autophagy-associated genes, such as *Atg5* or *Atg7*, impairs the self-renewal and hematopoietic reconstruction of HSC by increasing the accumulation of dysfunctional mitochondria and reactive oxygen species.[48] Furthermore, inhibition of autophagy repressed leukemia progress when the disease enters the maintenance phase.[49,50] However, the therapeutic approach targeting the enhanced autophagy in chemoresistant LSC to improve chemotherapy efficiency for AML treatment remains unexplored. Here, we found that autophagy upregulation was associated with chemotherapy recurrence in AML patient specimens. More importantly, inhibition of autophagy by a self-assembled leucine polymer dramatically enhanced the effect of DOX in eliminating LSC.

mTORC1 can phosphorylate and inactivate the autophagy mediators, such as ULK1, ATG13, AMBRA1, and ATG14L,[51] to suppress the autophagy initiation, autophagosome nucleation, and autophagy elongation.[52,53] Furthermore, mTORC1 promotes TFEB (transcription factor EB) nuclear entry to repress autophagy-associated genes.[54] It is known that DOX treatment can induce autophagy in cancer cells.[55] Consistently, we found that DOX treatment inactivated the mTORC1 pathway to stimulate autophagy in LSC enriched cells of AML mice. Leucine activates mTOR complex 1 (mTORC1) by directly destroying the mTORC1 repressor, Sestrin2-GATOR2 complex, and producing the metabolite acetyl-coenzyme A (AcCoA), which indirectly activates mTORC1.[56,57] Recent work shows that leucine directly activates SAR1B, a small GTPase, which undergoes a conformational change and dissociates from GATOR2, resulting in mTORC1 activation.[40] In line with this, we found that our newly developed self-assembled leucine polymer, 8L6, inhibited autophagy by activating mTORC1 in leukemic cells. Furthermore, Leu-DOX had enhanced the chemotherapeutic efficacy in eliminating functional LSC in AML than DOX treatment. We also found that this amino acid-based delivery system can release drugs in a low pH environment. Therefore, the high intracellular acidity in leukemic cells caused by high aerobic glycolysis[58] allowed Leu-DOX to specifically target leukemic cells and LSC in AML.

Overall, the bifunctional Leu-DOX, which inhibits autophagy and targets leukemic cells simultaneously, is a promising therapeutic approach for AML treatment.

Disclosures

No conflicts of interest to disclose.

Contributions

XX, Jian W, TT designed and performed most experiments and analyzed the data; WZ, WM, SW, and DZ contributed to animal experiments and patient sample assays; Jian W contributed to bioinformatics analysis; TT and Jun W contributed to nanocarriers; XX, MZ, and LJ wrote the paper; MZ, Jun W and LJ supervised the project.

Funding

We would like to thank the National Key Research and Development Program of China (grant numbers: 2018YFA0107200, 2017YFA0103403), the Key Research and Development Program of Guangdong Province (grant number: 2019B020234002), NSFC (grant numbers: 82170112, 52173150, 81900101, 81970139), Guangdong Introducing Innovative and Entrepreneurial Research Teams (grant number: 2019ZT08Y485), Guangdong Natural Science Funds for Distinguished Young Scholar (grant number: 2021B1515020012), Sanming Project of Medicine in Shenzhen (grant number: SZSM201911004), and Advanced Medical Technology Center, The First Affiliated Hospital, Zhongshan School of Medicine, Sun Yat-sen University for generous support.

Data-sharing statement

Data that support the findings of this study are available from the corresponding author upon reasonable request.

References

1. Klco JM, Mullighan CG. Advances in germline predisposition to acute leukaemias and myeloid neoplasms. Nat Rev Cancer. 2021;21(2):122-137.
2. Short NJ, Konopleva M, Kadia TM, et al. Advances in the treatment of acute myeloid leukemia: new drugs and new challenges. Cancer Discov. 2020;10(4):506-525.
3. Forte D, García-Fernández M, Sánchez-Aguilera A, et al. Bone marrow mesenchymal stem cells support acute myeloid leukemia bioenergetics and enhance antioxidant defense and escape from chemotherapy. Cell Metab. 2020;32(5):829-843.
4. Mercher T, Schwaller J. Corrigendum: pediatric acute myeloid leukemia (AML): from genes to models toward targeted therapeutic intervention. Front Pediatr. 2019;7:466.
5. Perloff M, Lesnick GJ, Korzun A, et al. Combination chemotherapy with mastectomy or radiotherapy for stage III breast carcinoma: a Cancer and Leukemia Group B study. J Clin Oncol. 1988;6(2):261-269.
6. Yang L, Li M, Wang F, et al. Ceritinib enhances the efficacy of substrate chemotherapeutic agent in human ABCB1-overexpressing leukemia cells in vitro, in vivo and ex-vivo. Cell Physiol Biochem. 2018;46(6):2487-2499.
7. Zhitnyak IY, Bychkov IN, Sukhorukova IV, et al. Effect of BN nanoparticles loaded with doxorubicin on tumor cells with multiple drug resistance. ACS Appl Mater Interfaces. 2017;9(38):32498-32508.
8. Mäkelä E, Pavic K, Varila T, et al. Discovery of a novel CIP2A variant (NOCIVA) with clinical relevance in predicting TKI resistance in myeloid leukemias. Clin Cancer Res. 2021;27(10):2848-2860.
9. Giacopelli B, Wang M, Cleary A, et al. DNA methylation epitypes highlight underlying developmental and disease pathways in acute myeloid leukemia. Genome Res. 2021;31(5):747-761.
10. Begna KH, Ali W, Naseema G, et al. Mayo Clinic experience with 1123 adults with acute myeloid leukemia. Blood Cancer J. 2021;11(3):46.
11. Park SM, Cho H, Thornton AM, et al. IKZF2 drives leukemia stem cell self-renewal and inhibits myeloid differentiation. Cell Stem Cell. 2019;24(1):153-165.
12. Pullarkat VA, Newman EM. BCL2 inhibition by venetoclax: targeting the Achilles' heel of the acute myeloid leukemia stem cell? Cancer Discov. 2016;6(10):1082-1083.
13. Crews LA, Balaian L, Delos Santos NP, et al. RNA splicing modulation selectively impairs leukemia stem cell maintenance in secondary human AML. Cell Stem Cell. 2016;19(5):599-612.
14. Zipeto MA, Court AC, Sadarangani A, et al. ADAR1 activation drives leukemia stem cell self-renewal by impairing Let-7 biogenesis. Cell Stem Cell. 2016;19(2):177-191.
15. Horigome Y, Ida-Yonemochi H, Waguri S, et al. Loss of autophagy in chondrocytes causes severe growth retardation. Autophagy. 2020;16(3):501-511.
16. Mizushima N, Komatsu M. Autophagy: renovation of cells and tissues. Cell. 2011;147(4):728-741.
17. Mortimore GE, Schworer CM. Induction of autophagy by amino-acid deprivation in perfused rat liver. Nature. 1977;270(5633):174-176.
18. Xia H, Green DR, Zou W. Autophagy in tumour immunity and therapy. Nat Rev Cancer. 2021;21(5):281-297.
19. Yu T, Guo F, Yu Y, et al. Fusobacterium nucleatum promotes chemoresistance to colorectal cancer by modulating autophagy. Cell. 2017;170(3):548-563.
20. Chen Y, Wu J, Liang G, et al. CHK2-FOXK axis promotes transcriptional control of autophagy programs. Sci Adv. 2020;6(1):eaax5819.
21. Sumitomo Y, Koya J, Nakazaki K, et al. Cytoprotective autophagy maintains leukemia-initiating cells in murine myeloid leukemia. Blood. 2016;128(12):1614-1624.
22. Palmeira dos Santos C, Pereira GJ, Barbosa CM, et al. Comparative study of autophagy inhibition by 3MA and CQ on Cytarabine induced death of leukaemia cells. J Cancer Res Clin Oncol. 2014;140(6):909-920.
23. Dossou AS, Basu A. The emerging Roles of mTORC1 in macromanaging autophagy. Cancers (Basel). 2019;11(10):1422.
24. Yu L, McPhee CK, Zheng L, et al. Termination of autophagy and reformation of lysosomes regulated by mTOR. Nature. 2010;465(7300):942-946.
25. Mitchener JS, Shelburne JD, Bradford WD, et al. Cellular autophagocytosis induced by deprivation of serum and amino acids in HeLa cells. Am J Pathol. 1976;83(3):485-492.
26. Jewell JL, Russell RC, Guan KL. Amino acid signalling upstream of mTOR. Nat Rev Mol Cell Biol. 2013;14(3):133-139.
27. Bonvini A, Coqueiro AY, Tirapegui J, et al. Immunomodulatory role of branched-chain amino acids. Nutr Rev. 2018;76(11):840-856.
28. Siddik MAB, Shin AC. Recent progress on branched-chain amino acids in obesity, diabetes, and beyond. Endocrinol Metab (Seoul). 2019;34(3):234-246.
29. Pankiv S, Clausen TH, Lamark T, et al. p62/SQSTM1 binds directly to Atg8/LC3 to facilitate degradation of ubiquitinated

protein aggregates by autophagy. J Biol Chem. 2007;282(33):24131-24145.
30. Krivtsov AV, Twomey D, Feng Z, et al. Transformation from committed progenitor to leukaemia stem cell initiated by MLL-AF9. Nature. 2006;442(7104):818-822.
31. Somervaille TC, Cleary ML. Identification and characterization of leukemia stem cells in murine MLL-AF9 acute myeloid leukemia. Cancer Cell. 2006;10(4):257-268.
32. Yan X, Sun Q, Ji J, et al. Reconstitution of leucine-mediated autophagy via the mTORC1-Barkor pathway in vitro. Autophagy. 2012;8(2):213-221.
33. Tsien C, Davuluri G, Singh D, et al. Metabolic and molecular responses to leucine-enriched branched chain amino acid supplementation in the skeletal muscle of alcoholic cirrhosis. Hepatology. 2015;61(6):2018-2029.
34. Eskandari S, Guerin T, Toth I, et al. Recent advances in self-assembled peptides: Implications for targeted drug delivery and vaccine engineering. Adv Drug Deliv Rev. 2017;110-111:169-187.
35. Casares S, Stan AC, Bona CA, et al. Antigen-specific downregulation of T cells by doxorubicin delivered through a recombinant MHC II-peptide chimera. Nat Biotechnol. 2001;19(2):142-147.
36. Suzuki H, Forrest AR, van Nimwegen E, et al. The transcriptional network that controls growth arrest and differentiation in a human myeloid leukemia cell line. Nat Genet. 2009;41(5):553-562.
37. Kauffman MK, Kauffman ME, Zhu H, et al. Fluorescence-Based Assays for Measuring Doxorubicin in Biological Systems. React Oxyg Species (Apex). 2016;2(6):432-439.
38. Zhang S, Liu X, Bawa-Khalfe T, et al. Identification of the molecular basis of doxorubicin-induced cardiotoxicity. Nat Med. 2012;18(11):1639-1642.
39. Makadia HK, Siegel SJ. Poly Lactic-co-Glycolic Acid (PLGA) as Biodegradable Controlled Drug Delivery Carrier. Polymers (Basel). 2011;3(3):1377-1397.
40. Chen J, Ou Y, Luo R, et al. SAR1B senses leucine levels to regulate mTORC1 signalling. Nature. 2021;596(7871):281-284.
41. Salik B, Yi H, Hassan N, et al. Targeting RSPO3-LGR4 signaling for leukemia stem cell eradication in acute myeloid leukemia. Cancer Cell. 2020;38(2):263-278.
42. Ueda K, Kumari R, Schwenger E, et al. MDMX acts as a pervasive preleukemic-to-acute myeloid leukemia transition mechanism. Cancer Cell. 2021;39(4):529-547.
43. Shivakumar P, Rani MU, Reddy AG, et al. A study on the toxic effects of Doxorubicin on the histology of certain organs. Toxicol Int. 2012;19(3):241-244.
44. Oleaga C, Bernabini C, Smith AS, et al. Multi-organ toxicity demonstration in a functional human in vitro system composed of four organs. Sci Rep. 2016;6:20030.
45. Pugazhendhi A, Edison T, Velmurugan BK, et al. Toxicity of Doxorubicin (Dox) to different experimental organ systems. Life Sci. 2018;200:26-30.
46. Ho TT, Warr MR, Adelman ER, et al. Autophagy maintains the metabolism and function of young and old stem cells. Nature. 2017;543(7644):205-210.
47. Zhang J, Randall MS, Loyd MR, et al. Mitochondrial clearance is regulated by Atg7-dependent and -independent mechanisms during reticulocyte maturation. Blood. 2009;114(1):157-164.
48. Lee IH, Kawai Y, Fergusson MM, et al. Atg7 modulates p53 activity to regulate cell cycle and survival during metabolic stress. Science. 2012;336(6078):225-228.
49. Karvela M, Baquero P, Kuntz EM, et al. ATG7 regulates energy metabolism, differentiation and survival of Philadelphia-chromosome-positive cells. Autophagy. 2016;12(6):936-948.
50. Smith AG, Macleod KF. Autophagy, cancer stem cells and drug resistance. J Pathol. 2019;247(5):708-718.
51. Kamada Y, Funakoshi T, Shintani T, et al. Tor-mediated induction of autophagy via an Apg1 protein kinase complex. J Cell Biol. 2000;150(6):1507-1513.
52. Kim J, Kundu M, Viollet B, et al. AMPK and mTOR regulate autophagy through direct phosphorylation of Ulk1. Nat Cell Biol. 2011;13(2):132-141.
53. Settembre C, Fraldi A, Medina DL, et al. Signals from the lysosome: a control centre for cellular clearance and energy metabolism. Nat Rev Mol Cell Biol. 2013;14(5):283-296.
54. Settembre C, Zoncu R, Medina DL, et al. A lysosome-to-nucleus signalling mechanism senses and regulates the lysosome via mTOR and TFEB. Embo j. 2012;31(5):1095-1108.
55. Cai Q, Wang S, Jin L, et al. Long non-coding RNA GBCDRlnc1 induces chemoresistance of gallbladder cancer cells by activating autophagy. Mol Cancer. 2019;18(1):82.
56. Son SM, Park SJ, Lee H, et al. Leucine signals to mTORC1 via its metabolite acetyl-coenzyme A. Cell Metab. 2019;29(1):192-201.
57. Nicklin P, Bergman P, Zhang B, et al. Bidirectional transport of amino acids regulates mTOR and autophagy. Cell. 2009;136(3):521-534.
58. Hao X, Gu H, Chen C, et al. Metabolic imaging reveals a unique preference of symmetric cell division and homing of leukemia-initiating cells in an endosteal niche. Cell Metab. 2019;29(4):950-965.